THE JOURNAL OF BIOLOGICAL CHEMISTRY VOL. 285, NO. 52, pp. 40864–40878, December 24, 2010

Novel Anti-carbohydrate Antibodies Reveal the Cooperative Function of Sulfated *N*- and *O*-Glycans in Lymphocyte Homing*[S]◆

Received for publication, July 21, 2010, and in revised form, September 7, 2010 Published, JBC Papers in Press, October 7, 2010, DOI 10.1074/jbc.M110.167296

Jotaro Hirakawa[‡], Koichiro Tsuboi[‡], Kaori Sato[‡], Motohiro Kobayashi[§], Sota Watanabe[‡], Atsushi Takakura[‡], Yasuyuki Imai[‡], Yuki Ito[¶], Minoru Fukuda[¶], and Hiroto Kawashima[‡‖1]

From the [‡]Laboratory of Microbiology and Immunology, and the Global Center of Excellence Program, School of Pharmaceutical Sciences, University of Shizuoka, Shizuoka 422-8526, Japan, the [§]Department of Molecular Pathology, Shinshu University Graduate School of Medicine, Matsumoto, 390-8621, Japan, the [¶]Glycobiology Unit, Sanford-Burnham Medical Research Institute, La Jolla, California 92037, and [‖]PRESTO, Japan Science and Technology Agency, Kawaguchi 332-0012, Japan

Cell surface glycans play pivotal roles in immune cell trafficking and immunity. Here we present an efficient method for generating anti-carbohydrate monoclonal antibodies (mAbs) using gene-targeted mice and describe critical glycans in lymphocyte homing. We immunized sulfotransferase GlcNAc6ST-1 and GlcNAc6ST-2 doubly deficient mice with sulfotransferase-overexpressing Chinese hamster ovary cells and generated two mAbs, termed S1 and S2. Both S1 and S2 bound high endothelial venules (HEVs) in the lymphoid organs of humans and wild-type mice, but not in those of doubly deficient mice. Glycan array analysis indicated that both S1 and S2 specifically bound 6-sulfo sialyl Lewis X and its defucosylated structure. Interestingly, S2 inhibited lymphocyte homing to peripheral lymph nodes by 95%, whereas S1 inhibited it by only 25%. S2 also significantly inhibited contact hypersensitivity responses and L-selectin-dependent leukocyte adhesion to HEVs. Immunohistochemical and Western blot analyses indicated that S1 preferentially bound sulfated *O*-glycans, whereas S2 bound both sulfated *N*- and *O*-glycans in HEVs. Furthermore, S2 strongly inhibited the *N*-glycan-dependent residual lymphocyte homing in mutant mice lacking sulfated *O*-glycans, indicating the importance of both sulfated *N*- and *O*-glycans in lymphocyte homing. Thus, the two mAbs generated by a novel method revealed the cooperative function of sulfated *N*- and *O*-glycans in lymphocyte homing and immune surveillance.

Complex carbohydrates play roles in a variety of biological processes, including differentiation, development, immunity, tumor metastasis, and protein quality control (1). To clarify the functions of complex carbohydrates *in vivo*, it is essential to determine when, where, and which complex carbohydrate chains are expressed in a particular biological setting of interest. For this purpose, anti-carbohydrate mAbs are particularly useful. However, it is difficult to establish anti-carbohydrate mAbs, largely because a wide variety of complex carbohydrates are intrinsically expressed in mice and rats, which are widely used to generate mAbs.

Some of the most well studied functions of complex carbohydrates in immunity are in immune cell trafficking. In particular, lymphocyte homing and recruitment to the peripheral lymph nodes (PLNs)[2] through a specialized endothelium called the high endothelial venule (HEV) have been extensively examined (2, 3). The homing receptor L-selectin, which is expressed on the surface of lymphocytes, specifically interacts with a unique complex carbohydrate structure known as 6-sulfo sialyl Lewis X (sialic acidα2–3Galβ1–4[Fucα1-3(sulfo-6)]GlcNAcβ1-R) (4, 5), which is present at the nonreducing terminus of various *O*-glycans and *N*-glycans (Fig. 1*A*). The essential role of this unique carbohydrate structure for lymphocyte homing was revealed mainly through studies using glycosyltransferase- or sulfotransferase-deficient mice. Studies using double-null mice deficient in fucosyltransferase (FucT)-IV and -VII revealed that the fucosylation of HEV ligands is critical for their interaction with L-selectin (6, 7). Studies with mice deficient in core 1 β1,3-*N*-acetylglucosaminyltransferase (C1β3GnT) and core 2 β1,6-*N*-acetylglucosaminyltransferase-I (C2GnT-I), which are involved in the biosynthesis of the *O*-glycan core structures required for the modification with 6-sulfo sialyl Lewis X (supplemental Fig. S1), showed that both *N*- and *O*-glycans are important in lym-

* This work was supported in part by National Institutes of Health Grant PO1CA71932 (to M. F.). This work was also supported by Grant-in-Aid for Scientific Research, Category (B) 21390023 and Grant-in-Aid for Scientific Research on Priority Areas, Dynamics of Extracellular Environments 20057022 from the Ministry of Education, Culture, Sports, Science and Technology, Japan (to H. K.), by the Takeda Science Foundation (to H. K.), and by a research fellowship from the Japan Society for the Promotion of Science (to J. H.).

◆ This article was selected as a Paper of the Week.

[S] The on-line version of this article (available at http://www.jbc.org) contains supplemental Table S1 and Figs. S1 and S2.

[1] To whom correspondence should be addressed: Laboratory of Microbiology and Immunology, School of Pharmaceutical Sciences, University of Shizuoka, 52-1 Yada, Shizuoka 422-8526, Japan. Tel.: 81-54-264-5710; Fax: 81-54-264-5715; E-mail: kawashih@u-shizuoka-ken.ac.jp.

[2] The abbreviations used are: PLN, peripheral lymph node; HEV, high endothelial venule; FucT, fucosyltransferase; C1β3GnT, core 1 β1,3-*N*-acetylglucosaminyltransferase; C2GnT-I, core 2 β1,6-*N*-acetylglucosaminyltransferase-I; GlcNAc6ST, *N*-acetylglucosamine-6-*O*-sulfotransferase; GlyCAM-1, glycosylation-dependent cell adhesion molecule-1; DKO, doubly deficient; LacNAc, *N*-acetyllactosamine; CHS, contact hypersensitivity; Neu5Ac, *N*-acetylneuraminic acid; Cmah, CMP-Neu5Ac hydroxylase; Neu5Gc, *N*-glycolylneuraminic acid; MLN, mesenteric lymph node; PP, Peyer's patch; E-PHA, *Phaseolus vulgaris* erythroagglutinin; AAA, *Aleuria aurantia* agglutinin; CMFDA, 5-chloromethylfluorescein diacetate; CMTMR, 5-(and-6)-(((4-chloromethyl)benzoyl)amino)tetramethylrhodamine; EGFP, enhanced GFP.

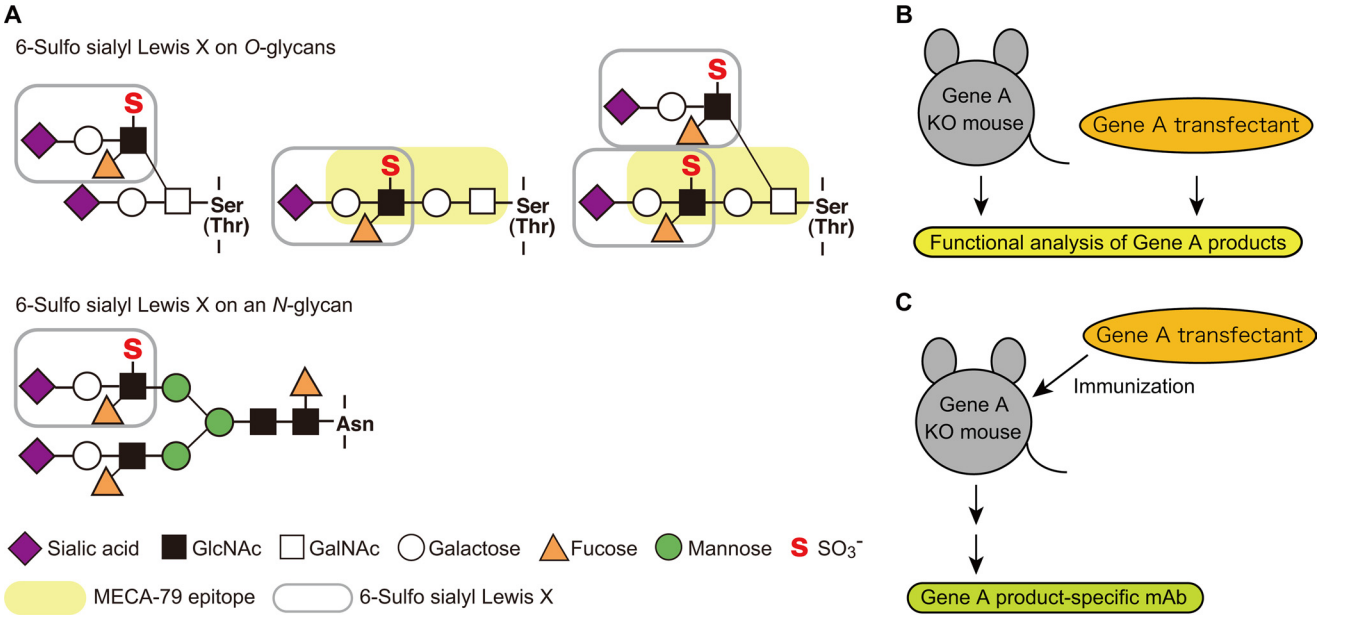

FIGURE 1. **Structures of the *O*- and *N*-glycans that are modified with 6-sulfo sialyl Lewis X structures, and a novel strategy for generating anti-carbohydrate mAbs.** *A*, 6-sulfo sialyl Lewis X structures on *O*- and *N*-glycans. Core 2 branched *O*-glycan (*upper left*), extended core 1 structure (*upper middle*), biantennary *O*-glycan containing both a core 2 branch and extended core 1 structure (*upper right*), and *N*-glycans (*bottom*) can be modified with 6-sulfo sialyl Lewis X (shown in *gray*). The extended core 1 structure modified with GlcNAc-6-*O*-sulfate (shown in *yellow*) is recognized by the mAb MECA-79 (16). *B*, functional analysis of glycogenes. Glycogene-deficient (*Gene A KO*) mice and glycogene-overexpressing transfectant cells have been widely used for functional analyses. *C*, a novel strategy for generating anti-carbohydrate mAbs. Glycogene-deficient mice are immunized with glycogene-overexpressing transfected cells. The carbohydrate structures formed by the glycogene-encoded enzyme are expected to be highly antigenic in glycogene-deficient mice.

phocyte homing and recruitment (8). However, it was not shown in those studies that sulfated *N*-glycans could indeed mediate lymphocyte homing, because specific probes against sulfated *N*-glycans were not available.

Our group (9) and others (10) previously generated mice deficient in two *N*-acetylglucosamine-6-*O*-sulfotransferases (GlcNAc6STs), GlcNAc6ST-1 and GlcNAc6ST-2 (also called HEC-GlcNAc6ST or L-selectin ligand sulfotransferase) and showed that GlcNAc-6-*O*-sulfation of the L-selectin ligand oligosaccharides expressed in HEVs plays a major role in recruiting lymphocytes to lymph nodes. In that work, we performed a detailed carbohydrate structural analysis of glycosylation-dependent cell adhesion molecule-1 (GlyCAM-1), which is specifically expressed in HEVs. After metabolically labeling the PLNs with [^{3}H]galactose in organ culture, we purified GlyCAM-1; released its *O*-glycans by β-elimination; purified each oligosaccharide by gel filtration, ion exchange chromatography, and HPLC; and determined the carbohydrate structure by exoglycosidase treatment and HPLC (summarized in supplemental Fig. S2*A*). Such carbohydrate structural analysis is essential in linking biological structure, and function. However, it is also laborious and time-consuming, especially when using biochemical methods to analyze carbohydrate structures expressed in a minor cell population, such as in HEVs. In this regard, anti-carbohydrate mAbs that react to a specific structure of interest would be very useful, because they can be used in immunohistochemistry, which provides information about the structure as well as the cell types in which the specific carbohydrate antigen is expressed.

The anti-carbohydrate mAb, MECA-79, which was generated by immunizing rats with a mouse PLN stromal cell fraction (11), has been widely used to detect HEVs in secondary lymphoid organs and HEV-like vessels at sites of chronic inflammation (4, 12) and has proved to be an extremely useful tool for determining the molecules involved in lymphocyte homing. MECA-79 binds various mucin-like glycoproteins called peripheral node addressins modified with L-selectin-reactive sulfated glycans in a sulfation-dependent manner (13, 14). However, MECA-79 only partially blocks L-selectin-dependent lymphocyte homing in functional studies (11). Furthermore, *O*-glycoprotease-resistant L-selectin ligands, distinct from the MECA-79 antigen, have also been detected (15). These findings can probably be explained by the fact that MECA-79 recognizes extended core 1 structures containing GlcNAc-6-*O*-sulfate (16), as shown in Fig. 1*A* and fails to bind core 2 branched *O*-glycans and *N*-glycans modified with 6-sulfo sialyl Lewis X, which are also recognized by L-selectin.

The purpose of this study was to develop an efficient method for generating anti-carbohydrate mAbs and to use the mAbs to determine critical glycan structures in lymphocyte homing. The strategy of the method we developed is schematically shown in Fig. 1 (*B* and *C*). Gene-targeted mice deficient in a certain glycogene, such as the glycosyltransferase or sulfotransferase gene (*gene A KO* in Fig. 1*B*), and glycogene-transfected cells have been extensively used for the functional analysis of complex carbohydrates (Fig. 1*B*). In the new method described here, the glycogene-deficient mice are immunized with transfected cells overexpressing the glycogene (Fig. 1*C*). Because the product of the glycogene-encoded enzyme should be highly antigenic in the glycogene-deficient mice, we hypothesized that anti-carbohydrate mAbs could be efficiently generated by this method.

In the present study, we immunized GlcNAc6ST-1 and GlcNAc6ST-2 doubly deficient (DKO) mice with transfected

cells expressing various glycosyltransferases and sulfotransferases, including GlcNAc6ST-2. As a result, we established two anti-carbohydrate mAbs, S1 and S2, which were reactive with HEVs in a sulfation-dependent manner. Although both of the mAbs specifically recognized α2,3-sialylated, GlcNAc-6-*O*-sulfated *N*-acetyllactosamine (LacNAc) terminal structure, S2 but not S1 strongly inhibited lymphocyte homing and contact hypersensitivity (CHS) responses. Further analyses revealed that S1 preferentially recognized sulfated *O*-glycans, whereas S2 recognized both sulfated *N*- and sulfated *O*-glycans in HEVs. These results indicate that sulfated *N*- and sulfated *O*-glycans function cooperatively in lymphocyte homing and immune surveillance.

EXPERIMENTAL PROCEDURES

Mice—GlcNAc6ST-1$^{-/-}$, GlcNAc6ST-2$^{-/-}$, FucT-IV$^{-/-}$-FucT-VII$^{-/-}$, GlcNAc6ST-1$^{-/-}$GlcNAc6ST-2$^{-/-}$, and C1β3GnT$^{-/-}$C2GnT-I$^{-/-}$ mice were backcrossed at least five generations to C57BL/6 WT mice and maintained as described previously (6, 8, 9). C57BL/6 WT and BALB/c Slc-nu/nu mice were purchased from Japan SLC (Hamamatsu, Japan). The mice were treated in accordance with the guidelines of the Animal Research Committee of the University of Shizuoka.

Establishment of Anti-sulfated Glycan mAbs—CHO cells stably expressing human CD34, human FucT-VII, human C1β3GnT, human C2GnT-I, and mouse GlcNAc6ST-2 (CHO/CD34/F7/C1/C2/GlcNAc6ST-2) were cultured in DMEM/F-12 medium (Sigma-Aldrich) supplemented with 10% FBS (HyClone) and penicillin-streptomycin (Invitrogen) and maintained in a humidified incubator (37 °C, 5% CO_2). CHO/CD34/F7/C1/C2/GlcNAc6ST-2 cells cultured in a 100-mm dish (BD) were transiently transfected with mouse CMP-*N*-acetylneuraminic acid (Neu5Ac) hydroxylase (Cmah), which generates CMP-*N*-glycolylneuraminic acid (Neu5Gc) from CMP-Neu5Ac (17), by FuGENE 6 transfection reagent (Roche Applied Science). After 48 h of transfection, the cells were washed with PBS and dispersed with 0.5 mM EDTA-PBS. After centrifugation, the cells were suspended in PBS and mixed with Imject Alum (Pierce) at a ratio of 1:1 in a final volume of 600 μl and vortexed vigorously for 30 min.

Two GlcNAc6ST-1 and GlcNAc6ST-2 DKO mice were immunized intraperitoneally three times at 2-week intervals with the cell suspension (250 μl/mouse). Four days after the final immunization, lymphocytes from the spleens of the two DKO mice were fused with P3X63Ag8.653 myeloma cells (American Type Culture Collection) in the presence of PEG solution (Sigma-Aldrich) and selected in the culture medium (RPMI 1640 medium (Invitrogen) supplemented with 15% FBS, penicillin-streptomycin, 50 μM 2-mercaptoethanol, and OPI (oxaloacetate, pyruvate, insulin) medium supplement (Sigma-Aldrich)) containing HAT (hypoxanthine, aminopterin, thymidine) supplement (Invitrogen) 24 h after fusion. The hybridoma supernatants that reacted with the HEVs of WT mice but not with those of GlcNAc6ST-1 and GlcNAc6ST-2 DKO mice were selected by immunofluorescence as described below. Hybridomas secreting anti-sulfated glycan mAbs thus selected were cloned by limiting dilution and adapted to the culture medium containing HT supplement (Invitrogen). The isotypes of the mAbs S1 and S2 were determined to be mouse IgM (κ) using an isotyping kit (GE Healthcare). Established clones were expanded and injected into BALB/c Slc-nu/nu mice (5.0×10^6 cells/mouse) that had been preinjected with 500 μl/mouse of pristane (2,6,10,14-tetramethyl pentadecane; Sigma-Aldrich) a few weeks before the cell injection, and the ascitic fluid was collected by standard procedures.

The S1, S2, and MECA-79 mAbs were purified from the ascites fluid using a Sephacryl S-300 (GE Healthcare) gel filtration column (1.5 × 100 cm) equilibrated with PBS. The fractions were collected at a flow rate of 12 ml/h, and the protein concentration in each fraction was determined using a BCA protein assay kit (Pierce). The fractions were subjected to SDS-PAGE on a 10% gel to examine the purity of the IgM. The purified IgM fraction (>95% purity) thus obtained was used for the following experiments. In some cases, purified antibodies were labeled with EZ-Link Sulfo-NHS-LC-Biotin (Pierce) according to the manufacturer's protocols.

Immunofluorescence—Acetone-fixed frozen sections (7-μm) from WT, KO, and DKO mice were incubated with PBS containing 3% BSA (Sigma-Aldrich) to block nonspecific binding sites and incubated with biotinylated S1, S2, or MECA-79 (BioLegend). After washing, the sections were incubated with 0.5 μg/ml streptavidin-Alexa Fluor 594 (Invitrogen) and mounted using Fluoromount (Diagnostic Biosystems). All of the images were obtained on a confocal laser scanning microscope (LSM510 META; Carl Zeiss, Inc.) using a 40× water immersion objective.

Transient Transfection and Flow Cytometry—CHO-K1 cells and two CHO cell-derived mutant lines, Lec1 and Lec2, were transiently transfected with pcDNA3.1/EGFP together with pcDNA3.1/mouse GlcNAc6ST-2 or pcDNA3.1/Zeo empty vector at a ratio of 1:20 using a pipette-type electroporator (Neon Transfection System; Invitrogen) according to the protocol provided by the manufacturer. In some experiments, mouse GlcNAc6ST-1 or mouse GlcNAc6ST-4 was transfected instead of mouse GlcNAc6ST-2. Forty-eight hours after transfection, the cells were washed with PBS, dispersed in 2 mM EDTA-PBS, and incubated with 1 μg/ml S1, S2, or MECA-79 (BD). After incubation with the mAbs, the cells were stained with biotin-conjugated goat anti-mouse IgM (1:500 dilution; Vector Laboratories; for S1 and S2) or 2.5 μg/ml biotin-conjugated mouse anti-rat IgM (BD; for MECA-79), followed by 0.5 μg/ml streptavidin-allophycocyanin (APC) conjugate (Beckman Coulter). For flow cytometric analysis of the CHO/CD34/F7/C1/C2/GlcNAc6ST-2 and CHO/CD34/F7/GlcNAc6ST-2 cell lines, the cells were incubated with purified S1, S2, or MECA79, followed by FITC-conjugated goat anti-mouse IgM (1:250 dilution, for S1 and S2; Vector Laboratories) or FITC-conjugated goat anti-rat IgM (1:500 dilution, for MECA-79; Open Biosystems). The cells were analyzed by flow cytometry on a FACSCanto II (BD). The data were acquired and analyzed with FACS Diva software (BD) and FlowJo software (Tree Star, Inc).

Lymphocyte Homing Assay—The lymphocyte homing assay was performed as described previously with some modifica-

tions (9, 18). Mesenteric lymph node lymphocytes and splenocytes from WT mice were labeled with 1 or 5 μM 5-chloromethylfluorescein diacetate (CMFDA; Invitrogen). After washing, 2.0×10^7 cells in 200 μl of PBS were injected intravenously into WT, GlcNAc6ST-1 and GlcNAc6ST-2 DKO, or C1β3GnT and C2GnT-I DKO mice. One hour after the injection, the number of $CMFDA^+$ cells in cell suspensions prepared from the recipient lymphoid organs was determined by flow cytometry. For the lymphocyte homing inhibition experiments, the mice were preinjected via the tail vein with purified S1, S2, or MECA-79 (200 μg/mouse) 2 h before the injection of CMFDA-labeled lymphocytes. The cells were analyzed by flow cytometry on a FACSCanto II or a FACSCalibur (BD). The data were acquired and analyzed as described above.

Contact Hypersensitivity—The CHS responses were measured as described previously with some modifications (9). In brief, 25 μl of 0.2% oxazolone (Sigma-Aldrich) in acetone: olive oil (4:1, v/v) was applied onto the shaved forelegs of mice on day 0. On days 0 and 3, 200 μl of 1 mg/ml mAbs in PBS or PBS alone was intraperitoneally injected. On day 5, the right ear was treated with 20 μl of 0.5% oxazolone (10 μl/side of the pinna), and the left ear was treated with vehicle. Ear swelling was measured using a thickness gauge before and 24 h after treatment. Paraffin-embedded tissue sections from the ears of the oxazolone-treated mice were stained with hematoxylin-eosin and observed using a BX-51 microscope (Olympus) with a 20× objective lens. Pictures were taken with a CCD camera, Penguin 600CL (Pixera).

Modified Stamper-Woodruff Cell Binding Assay—Leukocyte adhesion to HEVs was evaluated by the Stamper-Woodruff adhesion assay (19) with modifications, as follows: PLN cytosections (7-μm) on aminosilane-coated glass slides (Matsunami Glass Ind., Ltd.) were fixed for 10 min with PBS containing 0.5% glutaraldehyde (Wako Pure Chemicals). After three washes with distilled water, the nonspecific binding sites on the cytosections were blocked with buffer A (20 mM HEPES-NaOH, pH 7.4 150 mM NaCl, 1 mM $MgCl_2$, 1 mM $CaCl_2$) containing 3% BSA for 45 min. The sections were then incubated with or without 10 μg/ml MECA-79, purified S1 or S2, rat IgM (BioLegend), or mouse IgM (Rockland) in buffer A containing 0.1% BSA for 90 min at 4 °C. Freshly prepared leukocytes from the WT mouse spleens were labeled with 3.5 μM CellTracker Orange 5-(and-6)-(((4-chloromethyl)benzoyl)amino)tetramethylrhodamine (CMTMR; Lonza Walkersville, Inc.) for 10 min at 37 °C and suspended in 0.1% BSA in buffer A at a cell density of 1.0×10^7 cells/ml. The cells were preincubated in the presence or absence of 10 μg/ml MEL-14 (Beckman Coulter) or rat IgG (eBioscience) for 10 min on ice before being applied to glass slides. The CMTMR-labeled leukocytes were overlaid onto a glass slide (1.0×10^6 cells/section) and incubated for 30 min at 4 °C with rotation (60 rpm; Double shaker NR-3, TAITEC). After the removal of nonadherant cells by gentle tapping onto paper towels and dipping into buffer A in a 50-ml centrifuge tube (BD) for 10 s, the sections were fixed in buffer A containing 0.5% glutaraldehyde for 15 min at 4 °C. After three washes with distilled water, lymphocyte adhesion was quantified by fluorescence microscopy (Olympus BX51; 20× objective).

Leukocyte Rolling Assay—CHO/CD34/F7/C1/C2/GlcNAc6ST-2 cells cultured as monolayers in 35-mm culture dishes (Corning) were incubated with or without 10 μg/ml purified S1, S2, or MECA-79 for 10 min at room temperature. After incubation, the dishes were equipped with a parallel plate flow chamber (GlycoTech Co.), according to the manufacturer's instructions. Freshly prepared leukocytes from the spleens of WT mice were suspended in buffer A containing 0.1% BSA at 1×10^6 cells/ml and introduced into the flow chamber at a wall sheer stress of 2, 1.5, 1, and 0.5 dynes/cm^2 using a syringe pump Model 11 Plus (Harvard Apparatus Co.). For the L-selectin inhibition experiment, the leukocyte suspension was preincubated with 10 μg/ml MEL-14 for 10 min at 4 °C. Images were taken with a CCD camera (model ADT-40S; Flovel Co., Ltd.) equipped on an inverted microscope (Olympus CKX41; 20× objective).

Glycan Array Analysis—Glycan array analysis was performed at the Consortium for Functional Glycomics. Microarray slides (printed array version 4.1) containing 465 different glycans were used. In brief, the mAbs were diluted to 10 μg/ml in buffer B (20 mM Tris-HCl, pH 7.4 150 mM NaCl, 2 mM $CaCl_2$, 2 mM $MgCl_2$, 0.05% Tween 20) containing 1% BSA, applied to the printed surface of the array, and incubated at room temperature in a humidified chamber for 1 h. The microarray slide was rinsed four times in buffer B and four times in buffer B without Tween 20, and then fluorescently labeled anti-mouse IgM diluted in buffer B was added to the slide for 1 h. After washing as above, the slide was additionally washed four times with distilled water. Fluorescence intensities of the sample spots were measured using a ProScanArray Scanner (PerkinElmer Life Sciences).

Western Blotting—PLNs from WT, GlcNAc6ST-1 and GlcNAc6ST-2 DKO, or C1β3GnT and C2GnT-I DKO mice were dissected and suspended in PBS containing ice-cold 1% Triton X-100, and protease inhibitors (1:200 dilution; Sigma-Aldrich), and solubilized overnight with rotation at 4 °C. The lysates were centrifuged at 15,000 rpm for 10 min. The supernatants were collected, and their protein concentrations were determined using a BCA protein assay kit. The lysates thus obtained were stored at −80 °C until use. Western blotting was performed according to standard procedures using biotinylated S1, S2, MECA-79, and E-PHA (Seikagaku Kogyo Co.). The bands were detected with 0.5 μg/ml horseradish peroxidase-conjugated streptavidin (Vector Laboratories) and West Pico SuperSignal Chemiluminescent Substrate (Pierce).

Histological Examination of Human Tissues—The use of human tissue sections was approved by the Ethical Committee of Shinshu University School of Medicine. Tissue sections of human tonsil, chronic gastritis, and ulcerative colitis specimens of 3-μm thickness were deparaffinized in xylene and rehydrated in ethanol, and the antigens were retrieved by boiling the sections in 10 mM Tris-HCl buffer (pH 8.0) containing 1 mM EDTA for 20 min in a microwave oven. The endogenous peroxidase activity of the tissue was then quenched by soaking in absolute methanol containing 0.3% hydrogen peroxide for 30 min, and the nonspecific protein binding was

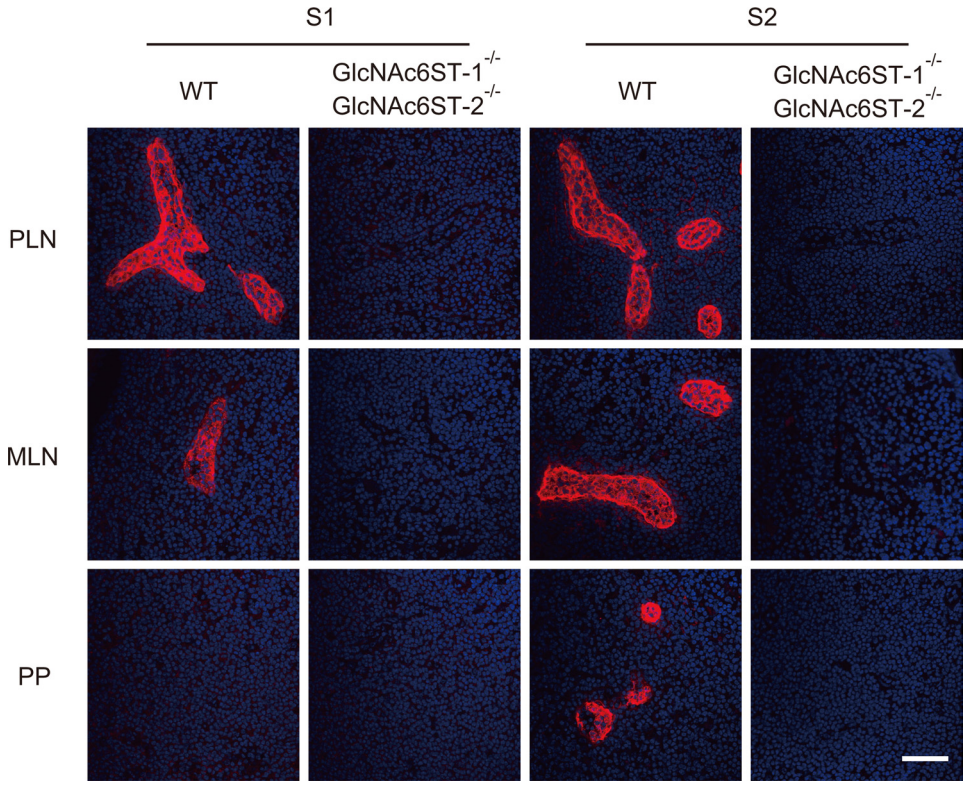

FIGURE 2. **Specific binding of S1 and S2 to sulfated glycans in HEVs.** Immunofluorescence of acetone-fixed frozen sections of PLNs, MLNs, and PPs from WT and GlcNAc6ST-1 and GlcNAc6ST-2 DKO mice reacted with S1 and S2 (*red*). Nuclear staining was performed with DAPI (*blue*). The data are representative of three independent experiments. *Bar*, 50 μm.

blocked with 1% BSA in TBS for 15 min. The sections were incubated with the MECA-79, S1, and S2 mAbs (5 μg/ml) with 5% BSA in TBS at 4 °C overnight. After washing in TBS, the sections were incubated with HRP-conjugated anti-rat Ig (Dako) diluted 1:100 with 5% BSA in TBS for 60 min for MECA-79 and with HRP- and anti-mouse Ig-conjugated polymer EnVision+ (Dako) for 30 min for the S1 and S2 mAbs. After washing in TBS, the color reaction was developed in TBS containing 0.2% 3,3′-diaminobenzidine (Dojindo), and 0.02% hydrogen peroxide for 7 min. The sections were briefly counterstained with hematoxylin. The slides were observed using an AX-80 microscope (Olympus) with a 100× oil immersion objective lens, and pictures were taken using a DP72 CCD camera (Olympus) with DP2-BSW software (Olympus).

Statistical Analysis—Student's *t* test was used for the determination of statistical significance between experimental groups. All of the results were expressed as the means ± S.D.

RESULTS

Generation of Anti-sulfated Glycan mAbs—A number of anti-sialyl Lewis X and anti-6-sulfo sialyl Lewis X mAbs have been reported (20, 21). However, as far as we know, none of these mAbs, except for MECA-79, reacts with the HEVs of C57BL/6 WT mice. This is probably because a large proportion of the terminal sialic acid in the WT mice is Neu5Gc, whereas these mAbs react with glycans modified with Neu5Ac (20). In addition, sialic acid is not a part of the glycan epitope for MECA-79 (16), which limits the utility of MECA-79 as a probe to detect the expression of L-selectin ligands, because sialic acid is required for L-selectin binding (22).

To obtain mouse tissue-reactive anti-sulfated glycan mAbs that recognize glycan epitopes more closely related to those that bind L-selectin than those recognized by MECA-79, CHO cells stably expressing CD34, FucT-VII, C1β3GnT, C2GnT-I, and GlcNAc6ST-2 (CHO/CD34/F7/C1/C2/GlcNAc6ST-2 cells) were transiently transfected with an expression vector encoding Cmah, which generates CMP-Neu5Gc from CMP-Neu5Ac (17). DKO mice deficient in two sulfotransferases, GlcNAc6ST-1 and GlcNAc6ST-2 (9), were immunized intraperitoneally with the resultant transfected cells, and the splenocytes of the immunized mice were used to generate hybridomas by cell fusion with a mouse myeloma line, P3X63Ag8.653. The culture supernatants were screened for their immunoreactivity with the HEVs of WT mice and for their lack of immunoreactivity with HEVs of the sulfotransferase DKO mice. As a result, two independent hybridoma clones, secreting anti-sulfated glycan mAbs S1 and S2 (mouse IgM, κ), were established. Immunofluorescence studies indicated that S1 selectively bound to the HEVs of PLNs and mesenteric lymph nodes (MLNs) but not to those of Peyer's patches (PPs) (Fig. 2). In contrast, S2 bound to the HEVs of PLNs, MLNs, and PPs. The immunoreactivity of these mAbs with HEVs was completely eliminated in the sulfotransferase DKO mice, indicating that they recognize sulfated glycans containing GlcNAc-6-*O*-sulfates.

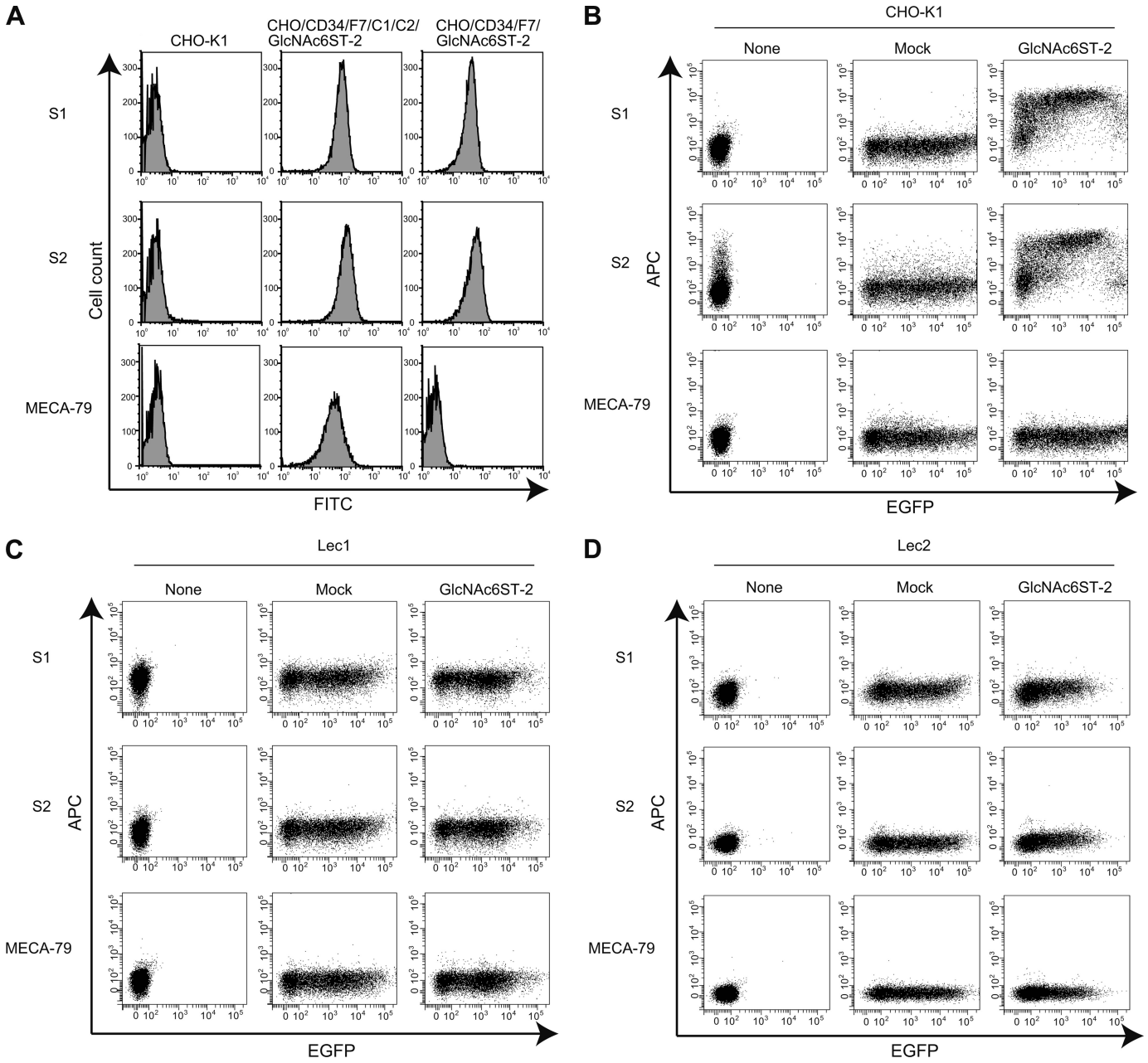

FIGURE 3. **Binding of S1 and S2 to sulfated and sialylated glycoproteins but not glycolipids.** *A*, parental CHO (CHO-K1), CHO/CD34/F7/C1/C2/GlcNAc6ST-2, and CHO/CD34/F7/GlcNAc6ST-2 cells were stained with purified S1, S2, or MECA-79 using FITC-conjugated secondary Abs. *B–D*, the GlcNAc6ST-2 gene was transiently transfected into CHO-K1 (*B*), Lec1 (*C*), or Lec2 (*D*) cells with a pcDNA3.1/EGFP expression vector. Forty-eight hours after transfection, the binding of S1, S2, and MECA-79 was determined by flow cytometry, as described under "Experimental Procedures." *None*, untransfected cells. *Mock*, cells mock-transfected with pcDNA3.1 empty vector together with the pcDNA3.1/EGFP expression vector. The data are representative of three (*A* and *B*) or two (*C* and *D*) independent experiments.

Flow cytometric analysis of CHO cells stably expressing various glycosyltransferases indicated that S1, S2, and MECA-79 clearly reacted with the CHO/CD34/F7/C1/C2/GlcNAc6ST-2 cells, which express CD34, FucT-VII, C1β3GnT, C2GnT-I, and GlcNAc6ST-2 (Fig. 3*A*). In contrast, S1 and S2 but not MECA-79 reacted with cells expressing CD34, FucT-VII, and GlcNAc6ST-2, but not C1β3GnT and C2GnT-I (CHO/CD34/F7/GlcNAc6ST-2) cells. These results indicate that the glycan epitopes for S1 and S2 are different from those of MECA-79, which recognizes extended core 1 structures containing GlcNAc-6-*O*-sulfate (16). The transient transfection of CHO cells with expression vectors encoding mouse GlcNAc6ST-2 and EGFP indicated that GlcNAc6ST-2 overexpression was sufficient to form the glycan epitopes for S1 and S2 (Fig. 3*B*). In addition, overexpression of either GlcNAc6ST-1 or GlcNAc6ST-4 alone could also form the glycan epitopes for these mAbs.[3]

CHO cells lack extended core 1 and core 2 structures because of a lack of C1β3GnT and C2GnTs (16, 23). In addition,

[3] J. Hirakawa, K. Tsuboi, and H. Kawashima, unpublished observations.

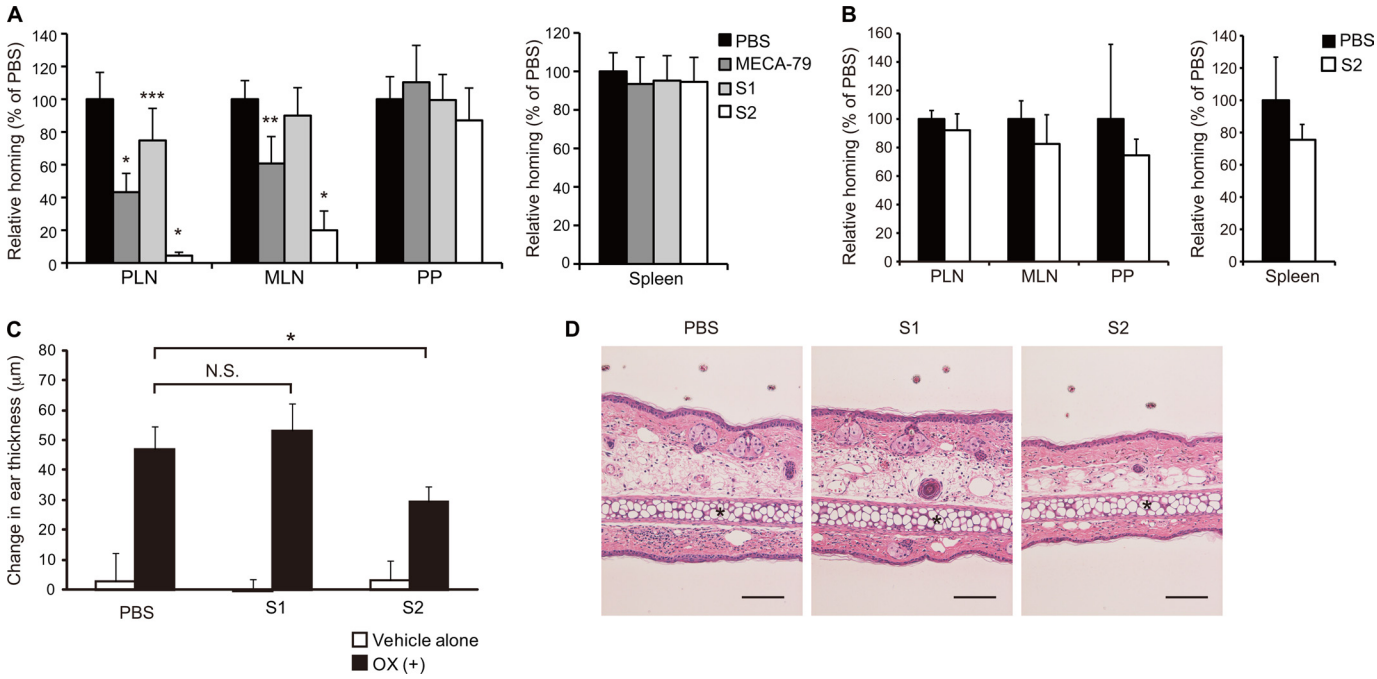

FIGURE 4. **Inhibition of lymphocyte homing and CHS responses by S2.** *A* and *B*, CMFDA-labeled lymphocytes (2.0×10^7 cells) were injected into the tail vein of WT (*A*) or GlcNAc6ST-1 and GlcNAc6ST-2 DKO mice (*B*). One hour after injection, CMFDA-labeled lymphocytes in lymphocyte suspensions from the PLNs, MLNs, PPs, and spleens were quantified by flow cytometry. The mice were preinjected with MECA-79, S1, or S2 (200 μg/mouse) or PBS 2 h before the injection of CMFDA-labeled lymphocytes. Lymphocyte homing to different lymphoid organs in the mAb-injected animals is shown as a percentage of that observed in PBS-injected animals, which was set as 100%. At least three recipient mice were used in each experiment. *, $p < 0.0001$; **, $p < 0.001$; ***, $p < 0.02$ *versus* PBS-injected control mice. *C*, ear swelling 24 h after challenge with oxazolone or vehicle alone in WT mice intraperitoneally injected twice with 200 μg/mouse of S1, S2, or PBS alone, as described under "Experimental Procedures." *Open bars*, change in thickness of the left ear treated with vehicle alone; *closed bars*, change in thickness of the right ear treated with oxazolone (*OX (+)*). *, $p < 0.01$; *N.S.*, not significant. $n = 4$. *D*, hematoxylin-and-eosin staining of ear sections 24 h after oxazolone challenge. *, ear cartilage. *Scale bar*, 100 μm. Each bar in *A–C* represents the means ± S.D. The data are representative of three (*A*) or two (*B–D*) independent experiments.

a CHO cell glycosylation mutant, Lec1, also lacks complex and hybrid type *N*-glycans because of a mutation of *N*-acetylglucosaminyltransferase-I (24) (summarized in supplemental Fig. S2*B*). However, these cells express glycolipids that might potentially serve as a substrate for GlcNAc6ST-2. As shown in Fig. 3*C*, Lec1 cells transfected with GlcNAc6ST-2 were not able to bind S1 and S2. In addition, Lec1 cells transfected with other sulfotransferases expressed in the HEVs in mice (9), GlcNAc6ST-1 and GlcNAc6ST-4, did not create S1- and S2-binding epitopes.[3] These results suggest two possibilities: (i) sulfated glycolipids cannot be formed by the GlcNAc6STs expressed in HEVs and/or (ii) S1 and S2 do not bind sulfated glycolipids even if they are formed. In either case, these results suggest that S1 and S2 bind the sulfated glycans on glycoproteins, but not those on glycolipids, in HEVs.

Under the same conditions, Lec2 cells, mutant CHO cells lacking the sialic acid modification because of the lack of CMP-sialic acid Golgi transporter (24) were also transfected with GlcNAc6ST-2 and EGFP expression vectors. However, no reactivity with S1 or S2 was detected (Fig. 3*D*), indicating that S1 and S2 recognize glycan epitopes containing GlcNAc-6-*O*-sulfate and sialic acid.

S2 Significantly Inhibited Lymphocyte Homing to PLNs and L-Selectin-mediated Adhesion—To assess the functional effects of the newly generated mAbs, we performed a lymphocyte homing assay. Interestingly, S2 inhibited the lymphocyte homing to PLNs by 95% in WT mice, whereas S1 inhibited it by only 25% (Fig. 4*A*). S2 also significantly inhibited the lymphocyte homing to MLNs, but not to PPs, possibly because interactions between $\alpha 4\beta 7$ integrin and MAdCAM-1 mainly mediate lymphocyte homing to PPs (25). S2 inhibited the lymphocyte homing to PLNs and MLNs more strongly than did MECA-79. The blocking ability of S2 appears to have been mediated by the recognition of sulfated glycans in the HEVs of WT mice, because the residual lymphocyte homing observed in the sulfotransferase DKO mice, which was 25% of that observed in WT mice (9), was not blocked by S2 (Fig. 4*B*).

To further examine the effects of the mAbs *in vivo*, we observed their effect on CHS responses. After oxazolone challenge, ear swelling and leukocyte infiltration during the sensitization phase were significantly blocked by treatment with S2 but not with S1 (Fig. 4, *C* and *D*). An immunohistochemical examination did not find any S2 staining in the ear after oxazolone challenge, whereas the HEVs of the draining lymph nodes showed strong positive staining.[3] Because S2 strongly blocked lymphocyte homing to the PLNs as described above, these results suggest that S2 alleviated CHS responses by blocking lymphocyte recruitment to the draining lymph nodes, not by blocking leukocyte trafficking to the sites of inflammation.

A modified Stamper-Woodruff cell binding assay indicated that S2 significantly inhibited the binding of fluorescently labeled leukocytes to the HEVs of lymph node tissue sections, similarly to the MECA-79 antibody (Fig. 5, *A* and *B*). S1 also slightly inhibited the binding, but the inhibition was not statistically significant. The binding observed in this assay was

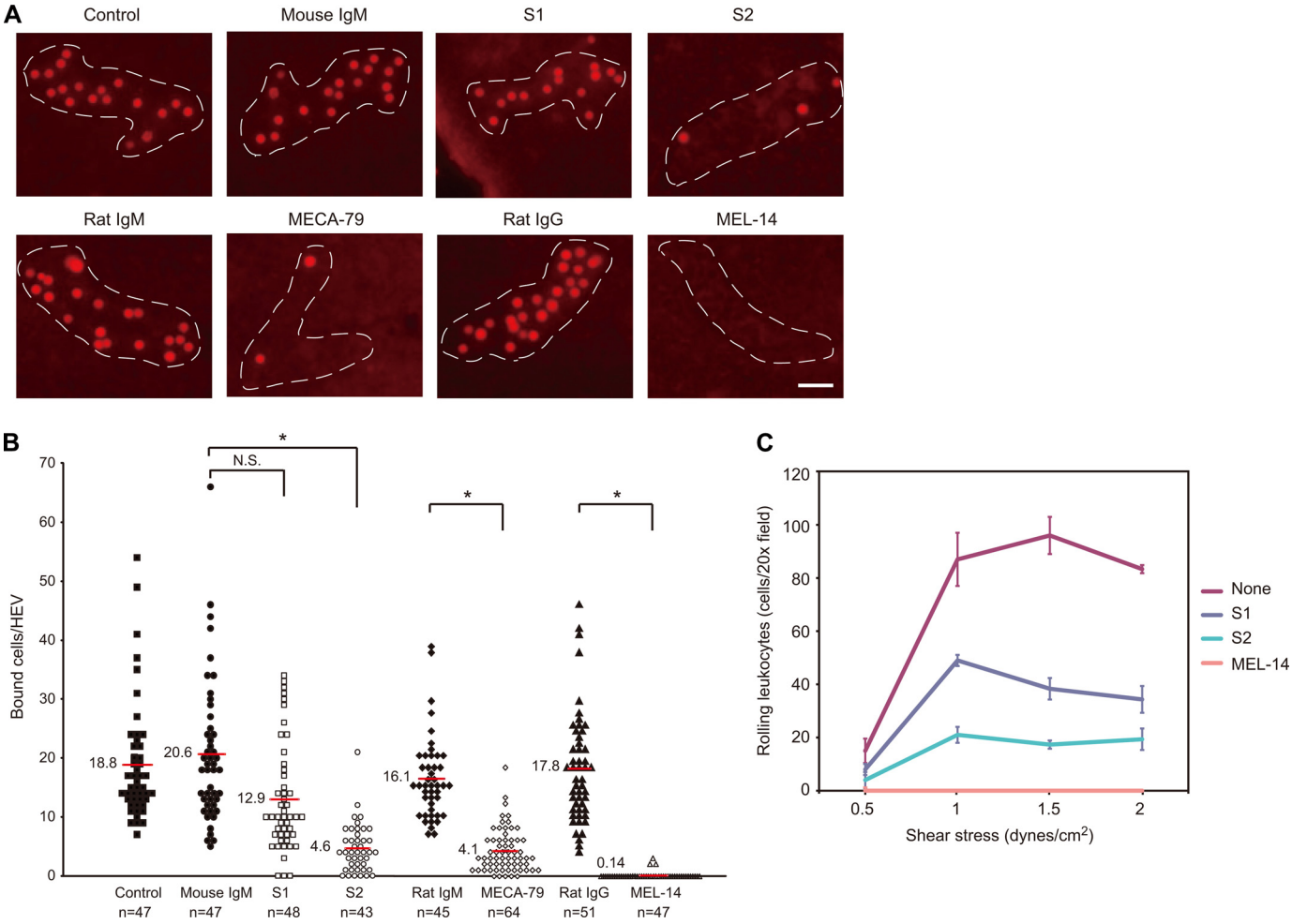

FIGURE 5. **Inhibition of the L-selectin-dependent adhesion of leukocytes to HEVs and leukocyte rolling by mAbs.** *A* and *B*, binding of CMTMR-labeled leukocytes incubated with or without 10 μg/ml rat IgG or MEL-14 to PLN tissue sections incubated with or without 10 μg/ml mouse IgM, S1, S2, rat IgM, or MECA-79. *A*, photomicrographs of leukocyte binding to HEVs. *Dotted lines*, outline of HEV. *Bar*, 40 μm. *B*, number of bound leukocytes per HEV. The number of cells bound to an HEV is plotted. The number of HEVs analyzed per sample (*n*) is indicated at the *bottom*. The *horizontal red lines* represent the average number of leukocytes bound per HEV. *N.S.*, not significant; *, $p < 0.001$. *C*, number of rolling leukocytes per 30 s on CHO transfectants stably expressing the 6-sulfo-sialyl Lewis X structure on *N*- and *O*-glycans (CHO/CD34/F7/C1/C2/GlcNAc6ST-2), pretreated with or without 10 μg/ml S1 or S2. Leukocytes applied to the flow chamber were treated with or without 10 μg/ml MEL-14. The data are representative of four (*A* and *B*) or three (*C*) independent experiments.

most likely dependent on L-selectin, because the anti-L-selectin mAb, MEL-14 (26), completely blocked the cell binding. Thus, these results suggest that S2 inhibited the interaction between L-selectin on leukocytes and its ligands on HEVs. To examine the ability of the newly generated mAbs to block L-selectin-mediated leukocyte rolling under physiological flow conditions, a parallel plate flow chamber assay was performed. As shown in Fig. 5*C*, CHO/CD34/F7/C1/C2/GlcNAc6ST-2 cells supported L-selectin-dependent leukocyte rolling under physiological shear stress. Consistent with the results of the lymphocyte homing assay, the rolling was markedly blocked by S2 by more than 80% and less effectively by S1.

Determination of Carbohydrate Structures Recognized by S1 and S2—We next sought to determine why only S2 strongly inhibited the lymphocyte homing and L-selectin-mediated adhesion of leukocytes to HEVs, even though both mAbs interacted with sulfated and sialylated glycans. To this end, we first examined the carbohydrate binding specificities of S1 and S2 by glycan array screening (Fig. 6 and supplemental Table S1). As shown in Fig. 6, both S1 and S2 interacted selectively with the 6-sulfo sialyl Lewis X structure (glycan 250) and its defucosylated structure, α2–3-sialylated 6-sulfo-LacNAc (glycan 249). The mAbs failed to interact with the unsulfated sialyl Lewis X structure (glycan 253) or α2–3-sialylated LacNAc (glycan 258), indicating that the sulfate group is required for their binding.

Consistent with flow cytometry results using Lec2 cells, sialic acid modification was also required for the mAb binding, because the unsialylated 6-sulfo Lewis X structure (glycan 288) did not show any interaction. α2–6-Sialylated 6-sulfo-LacNAc (glycan 265) did not bind to the mAbs, indicating that the sialic acid linkage to galactose should be α2–3. In addition, α2–3-sialylated 6-sulfated glycan bearing type I chain (glycan 236) did not react with the mAbs. Thus, the linkage between galactose and GlcNAc should be β1–4. The mAbs also did not bind the 6′-sulfo sialyl Lewis X structure (glycan 228), which was previously reported to interact with L-selectin (27); disulfated LacNAcs (glycan 34 and 295), whose molecular mimicry bound L-selectin (28); or α1–2 fucosylated 6-sulfo-LacNAc (glycan 219), which we previously reported to

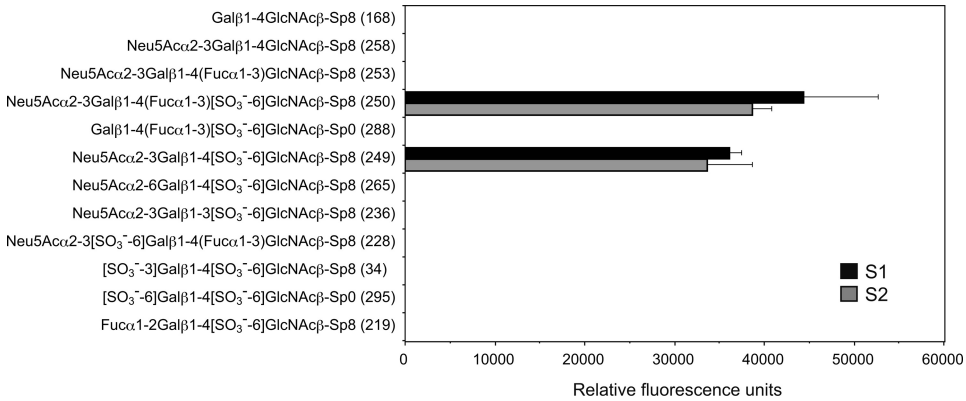

FIGURE 6. **Glycan array analysis of S1 and S2.** Version 4.1 of the printed array of the Consortium for Functional Glycomics was probed with 10 μg/ml S1 or S2. The *error bars* represent the means ± S.D. of four measurements. Glycan numbers are shown in the *parentheses* after their structures.

be present in the *O*-glycan moiety of mucins in the mouse colon (29, 30). Supplemental Table S1 shows the results of all 465 oligosaccharides displayed on the glycan array. None of the glycans (except glycan 249 and 250), including those with sulfates at various positions, interacted with the mAbs. Collectively, these results show that both S1 and S2 are highly specific for 6-sulfo sialyl Lewis X and its defucosylated structure.

S1 Preferentially Bound Sulfated O-Glycans, whereas S2 Bound Both Sulfated N- and Sulfated O-Glycans, in HEVs—The above results indicated that both S1 and S2 recognize the same glycan epitopes, whereas S2 showed a much higher ability to block lymphocyte homing and L-selectin-dependent leukocyte adhesion to HEVs. To clarify the reason for this apparent discrepancy, we next performed immunofluorescence staining using frozen sections of PLNs from various KO mice (Fig. 7*A*). Consistent with the results of the glycan array, S1 and S2 bound well to HEVs of the PLNs from FucT-IV and FucT-VII DKO mice (6). As expected, MECA-79 bound to the HEVs of fucosyltransferase DKO mice, whereas it failed to bind the HEVs of C1β3GnT and C2GnT-I DKO mice, which lack sulfated *O*-glycans (8). To our surprise, binding of S1 to the HEVs of C1β3GnT and C2GnT-I DKO mice was almost completely abolished compared with its binding to the HEVs of WT mice. However, clear binding of S2 to the HEVs of C1β3GnT and C2GnT-I DKO mice was still detected, although the staining intensity was slightly reduced. Furthermore, the binding of S1 to the HEVs of GlcNAc6ST-2 single KO mice was strongly diminished, whereas S2 binding was only slightly decreased (Fig. 7*A*). In addition, the binding of S1 and S2 to the HEVs of GlcNAc6ST-1 single KO mice was also slightly reduced. These results indicate that S1 preferentially binds *O*-glycans sulfated mainly by GlcNAc6ST-2 in HEVs, whereas S2 binds both *N*- and *O*-glycans sulfated by GlcNAc6ST-1 and GlcNAc6ST-2 in HEVs, consistent with the above results showing that S2 inhibits lymphocyte homing more strongly than S1.

To confirm that S2 could interact with both *N*- and *O*-glycans expressed in HEVs, PLN tissue sections of WT and C1β3GnT and C2GnT-I DKO mice were treated with *N*-glycosidase F, which cleaves *N*-glycans, and then the ability of the mAbs to bind the sections was examined (Fig. 7*B*). The binding of *Phaseolus vulgaris* erythroagglutinin (E-PHA), a lectin that preferentially binds to *N*-glycans bearing a bisecting GlcNAc (31), was significantly diminished after the enzyme treatment, whereas that of MECA-79 was unaffected, indicating that the *N*-glycans were specifically cleaved from the tissue sections after the enzyme treatment. After *N*-glycosidase F treatment, the binding of S2 to the HEVs of WT mice was markedly decreased, although not completely abrogated; this suggests that S2 bound to the remaining *O*-glycans after the enzyme treatment. Furthermore, S2 binding to the HEVs of C1β3GnT and C2GnT-I DKO mice was almost completely eliminated after *N*-glycosidase F treatment. Collectively, these results indicate that S2 binds both sulfated *N*- and sulfated *O*-glycans expressed in HEVs, whereas S1 preferentially binds sulfated *O*-glycans in HEVs, consistent with the results that S2 showed much a higher ability to block lymphocyte homing than S1.

S2 Bound L-Selectin Ligand Glycoproteins in a Sulfated N- and Sulfated O-Glycan-dependent Manner—To determine which glycoproteins are reactive with the newly generated mAbs, we next performed Western blot analyses using tissue lysates prepared from the PLNs of WT and sulfotransferase DKO mice (Fig. 8*A*). MECA-79 reacted with glycoproteins with molecular sizes of >200, 170, 90, and 55–60 kDa, which most likely were the known L-selectin-binding proteins Sgp200, podocalyxin-like protein, CD34, and GlyCAM-1 (4), respectively. In the Western blot, no bands were detected with S1 even at a high concentration, 5 μg/ml.[3] S2 clearly reacted with PLN glycoproteins with molecular sizes of >200, 170, and 90 kDa. Interestingly, however, the binding of S2 to the 55–60-kDa glycoprotein could not be detected, although a very faint band could be detected after long exposure.[3] The binding of S2 to the PLN glycoproteins was completely eliminated in the sulfotransferase DKO mice, confirming that the binding is sulfation-dependent.

We next examined the effects of *N*-glycosidase F on the binding of S2 to the glycoprotein species in Western blots. After *N*-glycosidase F treatment, the binding of E-PHA was markedly reduced, whereas that of MECA-79 appeared unaffected, confirming that *N*-glycosidase F specifically cleaved the *N*-glycans. After the enzyme treatment, the binding of S2 to the PLN glycoproteins from WT mice was

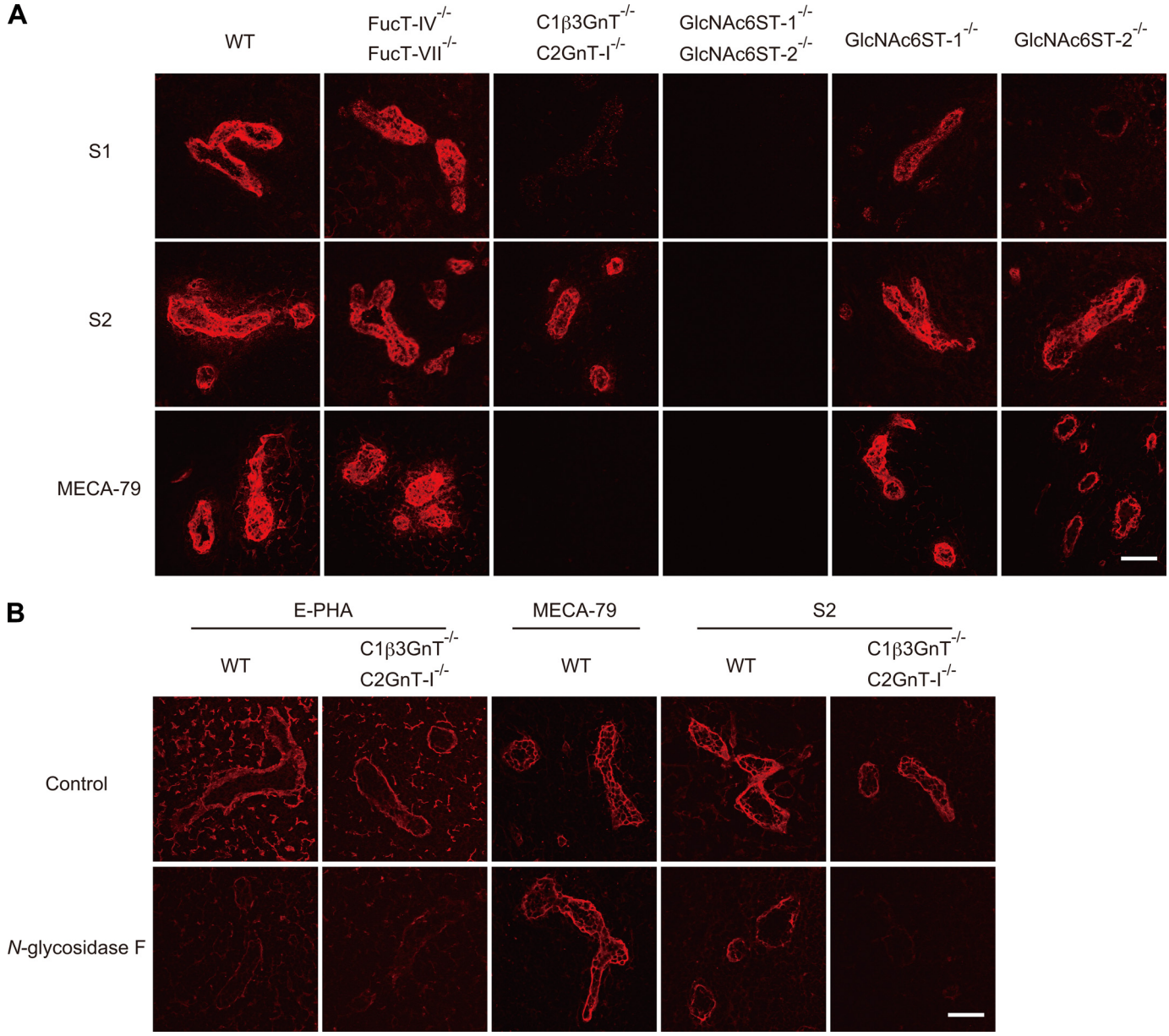

FIGURE 7. **Binding of mAbs to PLN sections from various gene-targeted mice.** *A*, frozen sections (7 μm) of PLNs from WT, FucT-IV, and FucT-VII DKO, C1β3GnT and C2GnT-I DKO, GlcNAc6ST-1 and GlcNAc6ST-2 DKO, GlcNAc6ST-1-deficient, and GlcNAc6ST-2-deficient mice were incubated with 5 μg/ml biotinylated S1, S2, or MECA79 for 2 h (*red*). *B*, effects of *N*-glycosidase F treatment on the binding of mAbs or E-PHA to HEVs. Frozen sections from the PLNs of WT and C1β3GnT and C2GnT-I DKO mice were fixed with cold acetone and treated for 24 h at 37 °C with or without 100 milliunits/ml *N*-glycosidase F (Calbiochem) in 10 mM HEPES-NaOH (pH 7.4), 0.1% Triton X-100, and complete protease inhibitor (Roche Applied Science) and incubated with biotinylated E-PHA (0.1 μg/ml), MECA-79 (1 μg/ml), or S2 (1 μg/ml) for 1 h. The binding of biotinylated E-PHA and mAbs was detected with Alexa Fluor 594-conjugated streptavidin using a confocal laser scanning microscope (LSM510 META). *Bar*, 50 μm. The data are representative of four (*A*) or three (*B*) independent experiments.

diminished by ~50% (Fig. 8*B*). Furthermore, S2 weakly bound to five glycoproteins with molecular sizes from 100 to >200 kDa in the PLN lysates from C1β3GnT and C2GnT-I DKO mice, which may represent Sgp200 and some other glycoprotein species lacking extended core 1 and core 2 *O*-glycans. S2 binding to these glycoproteins was completely eliminated by *N*-glycosidase F treatment. Collectively, these results indicate that the binding of S2 to L-selectin ligand glycoproteins is dependent on both sulfated *N*- and sulfated *O*-glycans.

S2 Significantly Inhibited the N-Glycan-dependent Lymphocyte Homing to PLNs in C1β3GnT and C2GnT-I DKO Mice—The above results indicated that S1 preferentially bound sulfated *O*-glycans, whereas S2 bound both sulfated *N*- and sulfated *O*-glycans in HEVs. These results suggest that both sulfated *N*- and *O*-glycans play critical roles for lymphocyte homing. To confirm the importance of sulfated *O*-glycans in lymphocyte homing, a short term homing assay using WT and C1β3GnT and C2GnT-I DKO mice, which lack sulfated *O*-glycans (8), was performed. The lymphocyte homing to PLNs in C1β3GnT and C2GnT-I DKO mice was diminished by ~60% compared with that in WT mice in our assay (Fig. 9*A*), consistent with previous findings (8), confirming that *O*-glycans are important for lymphocyte homing to PLNs. To determine the importance of sulfated *N*-glycans in lymphocyte homing, we next examined whether S2 could inhibit the

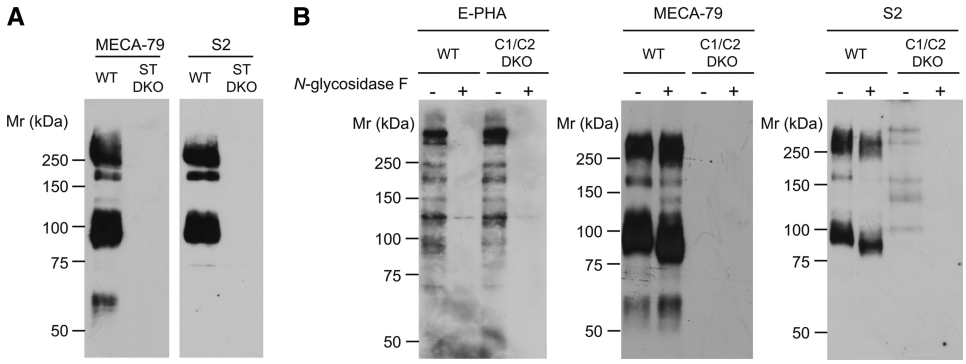

FIGURE 8. **Western blot analysis of PLN lysates with S2 and MECA-79.** *A*, immunoblot of lysates (20 μg) from WT or GlcNAc6ST-1 and GlcNAc6ST-2 DKO (ST DKO) mice probed with 0.5 μg/ml biotinylated MECA-79 or -S2. *B*, immunoblot of lysates from WT or C1β3GnT and C2GnT-I DKO (C1/C2 DKO) mice treated with buffer alone (−) or with *N*-glycosidase F (+) probed with 0.5 μg/ml biotinylated E-PHA, -MECA-79, or -S2. *N*-glycosidase F treatment (100 units/ml; Roche Applied Science) was performed in PBS containing 0.9% Triton X-100 and a protease inhibitor mixture (1:40 dilution; Sigma-Aldrich) for 2 h at 37 °C. Ten micrograms of lysate proteins were applied to each lane, except that 100 μg of lysate proteins from the C1β3GnT and C2GnT-I DKO mice were applied for the blot with S2. The data are representative of three independent experiments.

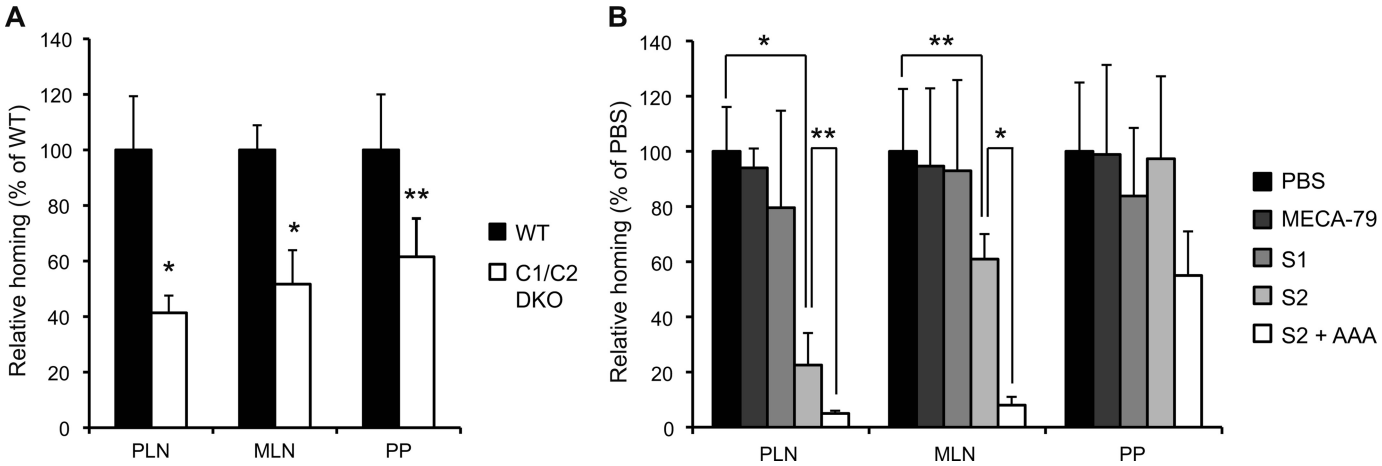

FIGURE 9. **Inhibition of *N*-glycan-dependent lymphocyte homing by S2.** *A*, CMFDA-labeled lymphocytes (2.0×10^7 cells) were injected into the tail vein of WT or C1β3GnT and C2GnT-I DKO mice (C1/C2 DKO), and the lymphocyte homing to different lymphoid organs is shown as a percentage of that observed in WT mice, which was set as 100%. Three to four recipient mice were used in each experiment. *, $p < 0.005$; **, $p < 0.03$. *B*, CMFDA-labeled lymphocytes (2.0×10^7 cells) were injected into the tail vein of C1β3GnT and C2GnT-I DKO mice. One hour after injection, CMFDA-labeled lymphocytes in the lymphocyte suspensions from PLNs, MLNs, and PPs were quantified by flow cytometry. The C1β3GnT and C2GnT-I DKO mice were preinjected with 200 μg/mouse of MECA-79, S1, S2, or PBS 2 h before the injection of CMFDA-labeled lymphocytes. In some cases (S2 + AAA), C1β3GnT and C2GnT-I DKO mice were preinjected with 200 μg/mouse of S2 together with 100 μg/mouse of AAA lectin (Seikagaku Kogyo Co.) before the injection of CMFDA-labeled lymphocytes. Lymphocyte homing to different lymphoid organs in the mAb-injected animals is shown as a percentage of that observed in PBS-injected animals, which was set as 100%. Three to four recipient mice were used in each experiment. *, $p < 0.001$; **, $p < 0.025$. The data are representative of two independent experiments.

residual lymphocyte homing in C1β3GnT and C2GnT-I DKO mice. As expected, MECA-79 did not show any inhibitory activity. In contrast, S2 inhibited residual lymphocyte homing to PLNs in the C1β3GnT and C2GnT-I DKO mice by 80%, whereas S1 did not show any inhibitory activity (Fig. 9*B*). These results indicate that the sulfated *N*-glycans expressed in the HEVs mediate the residual lymphocyte homing in C1β3GnT and C2GnT-I DKO mice. S2 failed to inhibit lymphocyte homing to PPs, possibly because interactions between α4β7 integrin and MAdCAM-1 play a critical role in lymphocyte homing to PPs (25) as described above. Furthermore, the co-administration of a fucose-specific lectin *Aleuria aurantia* agglutinin (AAA) with S2 blocked the lymphocyte homing to PLN in C1β3GnT and C2GnT-I DKO mice by more than 95%, suggesting that the unsulfated sialyl Lewis X structure on *N*-glycans mediated the residual L-selectin ligand activity after S2 treatment. Taken together, these results indicate that sulfated *N*- and *O*-glycans function cooperatively in lymphocyte homing and that S2 inhibits the function of both types of glycans.

Histological Examination of Ectopic Human Lymphoid Organs by S1 and S2—To determine whether S1 and S2 could be used as a probe to detect the HEV-like blood vessels formed at chronic disease sites in humans, we performed immunohistochemical staining of human pathology samples (Fig. 10). We first immunostained human tonsil tissue sections with the S1 and S2 mAbs, using MECA-79 as a positive control. The HEVs in tonsil tissue reacted well with both S1 and S2, whose signals were almost equivalent to that of MECA-79. To determine whether the S1 and S2 mAbs also bound to the HEV-like vessels induced in chronic inflammatory states, which are reactive with MECA-79, we performed immunohistochemistry using sections from human tissue specimens of chronic *Helicobacter pylori* gastritis (32) and ulcerative colitis (33). The results showed that the HEV-like vessels induced in the gastrointestinal lamina propria, particularly in and around the

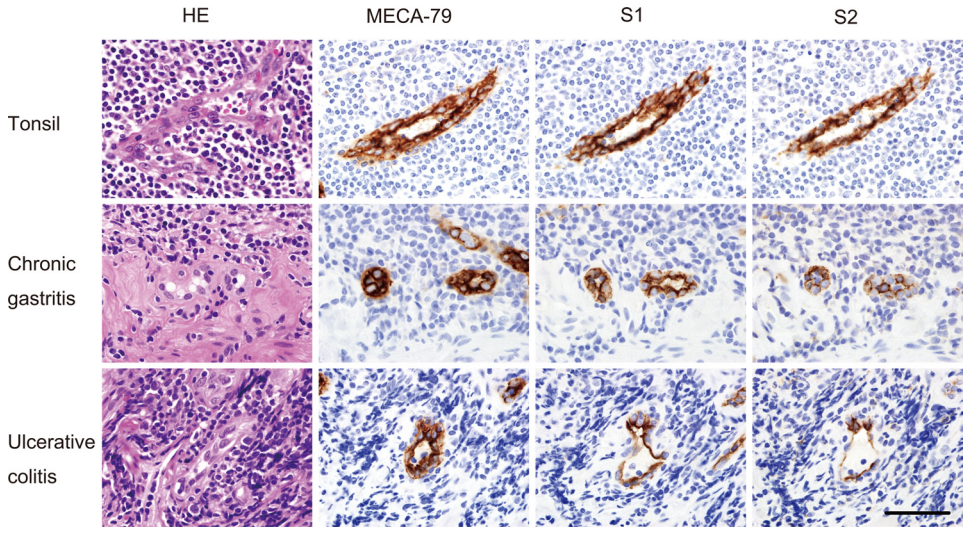

FIGURE 10. **Immunohistochemistry of human tissue sections with the MECA-79, S1, and S2 mAbs.** HEVs in the human tonsil were stained well with the MECA-79, S1, and S2 mAbs (*top row*). HEV-like vessels induced in the gastrointestinal lamina propria, particularly in and around the muscularis mucosae, in chronic *H. pylori* gastritis (*middle row*) and ulcerative colitis (*bottom row*) specimens also showed positive signals. *Bar*, 50 μm. The data are representative of two independent experiments.

muscularis mucosae, reacted well with both mAbs. These results indicate that the sulfated glycans expressed not only on normal HEVs of human secondary lymphoid organs but also those expressed on the HEV-like vessels induced in nonlymphoid tissues in pathological settings contain the epitopes for S1 and S2.

DISCUSSION

In the present study we developed an efficient method for generating anti-carbohydrate mAbs, by immunizing glycogene-deficient mice with transfected CHO cells that overexpress the glycan epitopes formed by the glycogenes. As an example, we immunized sulfotransferase-deficient mice and successfully developed two mAbs, termed S1 and S2. We showed that both of them specifically recognized α2,3-sialylated 6-sulfo LacNAc and 6-sulfo sialyl Lewis X structures as minimum epitopes. Interestingly, S2 but not S1 significantly blocked lymphocyte homing and CHS responses. Further analysis using C1β3GnT and C2GnT-I DKO mice indicated that S1 preferentially recognized sulfated *O*-glycans, whereas S2 bound both sulfated *N*- and *O*-glycans in HEVs, indicating that both sulfated *N*- and *O*-glycans play pivotal roles in lymphocyte homing.

Over the past few decades, most of the glycogenes encoding glycan-modifying enzymes, such as glycosyltransferases and sulfotransferases, have been identified. Extensive *in vivo* functional analyses of complex carbohydrates using glycogene loss-of-function mutants (*Gene A KO* in Fig. 1, *B* and *C*) and *in vitro* functional analyses using transfectant cells with a glycogene gain-of-function phenotype have been performed. Thus, a number of gene-targeted mice deficient in various glycogenes are now available. The concept behind the method we developed in this study is quite simple: using these mutant mice as tools, we immunize them with transfected cells overexpressing the missing glycogenes. Because the products of the glycogene-encoded enzyme should be highly antigenic in the glycogene-deficient mice, we hypothesized that anti-carbohydrate mAbs could be efficiently generated by this method. The generation of anti-bisecting GlcNAc antisera in *N*-acetylglucosaminiyltransferase III-deficient mice immunized with mutant LEC10 CHO cells expressing this glycosyltransferase caused by the activation of the endogenous gene was previously reported (34). In addition, the generation of anti-Neu5Gc antisera in Cmah-deficient mice immunized with thymocytes from WT mice, which express Neu5Gc, was also reported (35). However, these studies did not try to generate mAbs, which should serve as much more specific probes for glycans. In contrast, we generated anti-carbohydrate mAbs based on the idea described above. We used transfected cells as an immunogen because it is easy to modify their carbohydrate structures by introducing additional cDNAs that encode glycan-modifying enzymes. As described above, by transfecting sulfotransferase-expressing cells with Cmah to modify the terminal sialic acid, we successfully generated mAbs that were reactive with mouse tissues rich in Neu5Gc (20). Because the cDNAs of various glycan-modifying enzymes and a number of mutant mice deficient in glycosyltransferases and sulfotransferases are now available, we believe that our method established here will be widely applicable for the generation of various anti-carbohydrate mAbs.

Our glycan array analysis showed that both of the mAbs were highly specific to α2,3-sialylated 6-sulfo LacNAc and 6-sulfo sialyl Lewis X as minimum structures. However, our results also showed that S1 preferentially bound sulfated *O*-glycans, whereas S2 bound both sulfated *N*- and sulfated *O*-glycans in HEVs. Similar to S1, MECA-79, which recognizes extended core 1 structures modified with sulfate (16), did not bind *N*-glycans in HEVs. However, we think that the reason for this lack of binding is fundamentally different for S1 and MECA-79, because the extended core 1 structure is a part of the binding epitope for MECA-79 (16), whereas the terminal 6-sulfo sialyl Lewis X structure is the binding epitope for S1,

as revealed by our glycan array analysis. Why do S1 and S2 differentially bind to the *N*- and *O*-glycans expressed in HEVs? One possible explanation is that S1 binds to these glycans when they are clustered, whereas S2 binds to them even when they are sparse, because multiple *O*-glycans are present on sialomucins expressed in HEVs (4). Consistent with this idea, not only S2 but also S1 could bind to overexpressed sulfated *N*-glycans, which was shown by the experiment that the transfection of CHO cells with GlcNAc6ST-2 cDNA using an expression vector with a strong cytomegalovirus promoter conferred on the cells a reactivity to both S1 and S2.

In our Western blot analysis, S2 preferentially bound glycoprotein species of >200, 170, and 90 kDa, which were probably Sgp200, podocalyxin-like protein, and CD34, respectively (4). Interestingly, however, S2 bound very weakly to a 55–60-kDa glycoprotein likely representing GlyCAM-1, which is modified with sulfated *O*-glycans but not *N*-glycans (36). GlyCAM-1-deficient mice are reported to have normal lymphoid organ architecture and normal lymphocyte homing into PLNs (37). In addition, GlyCAM-1 is recovered not only from the membrane fraction but also from the culture supernatant of lymph node organ culture (38). These findings suggest that GlyCAM-1 functions as a modulator of lymphocyte homing by competing with membrane-bound L-selectin ligands. In this regard, it is notable that S2 bound well to the other three glycoprotein species that serve as membrane-bound L-selectin ligands. Why did S2 fail to bind well to the 55–60-kDa glycoprotein? One possible reason is that both *N*- and *O*-glycans are required for glycoprotein species to interact with S2 in Western blots, because GlyCAM-1 is modified only by *O*-glycans (36). However, we cannot exclude the possibility that some other factors including core protein preference of the mAb might be involved, because *N*-glycosidase F treatment of the PLN lysates only partially reduced the binding of S2 to >200-, 170-, and 90-kDa glycoproteins in our Western blots. In addition, our results also showed that the relative contributions of *N- versus O*-glycans to the S2 binding appear to differ in immunohistochemistry and Western blots, because significant binding of S2 to HEVs in C1β3GnT and C2GnT-1 DKO mice could be detected in immunohistochemistry, whereas only a weak binding of S2 to glycoproteins from PLN lysates from these mutant mice were detected in Western blots. In both of these experiments, however, *N*-glycosidase F treatment led to the same conclusion that S2 bound both *N*- and *O*-glycans expressed in HEVs.

One may argue that the importance of *N*-glycans in lymphocyte homing was already shown by studies using C1β3GnT and C2GnT-I DKO mice (8). However, it was not shown in that report that sulfated *N*-glycans could mediate lymphocyte homing, because specific probes against sulfated *N*-glycans were not available. Instead, *N*-glycan-specific lectins were used to show the importance of *N*-glycans in lymphocyte homing. In the present study, by using specific mAbs, we provide clear evidence that sulfated *N*-glycans play a critical role in lymphocyte homing. We also showed that the residual homing observed in C1β3GnT and C2GnT-I DKO mice after treatment with S2 was significantly blocked by AAA lectin, which binds fucose, suggesting that *N*-glycans modified with unsulfated sialyl Lewis X could support the remaining lymphocyte homing. However, because most of the lymphocyte homing to the PLNs in C1β3GnT and C2GnT-I DKO mice was blocked by S2, we think that sulfated *N*-glycans play a major role in lymphocyte homing in these mice.

As far as we know, no previous study has assessed the relative importance of GlcNAc6ST-1 and GlcNAc6ST-2 in the sulfation of *N- versus O*-glycans in HEVs. Our results suggest that these two GlcNAc6STs are differentially involved in the formation of the epitopes for S1 and S2. The binding of S1 to the HEVs of PLNs was largely dependent on GlcNAc6ST-2, whereas that of S2 was dependent on both GlcNAc6ST-1 and GlcNAc6ST-2, as revealed by immunofluorescence studies. Considering the *N*- and *O*-glycan preference of these mAbs, these results suggest that GlcNAc6ST-2 may be more important for *O*-glycan sulfation in HEVs than GlcNAc6ST-1, and GlcNAc6ST-1 may be more important for *N*-glycan sulfation in HEVs than GlcNAc6ST-2. Consistent with this idea, previous acceptor specificity studies of GlcNAc6ST-2 showed that it transfers sulfate more readily to core 2 *O*-glycans than to *N*-glycans (39). In addition, our results indicated that S2 but not S1 bound the HEVs of PPs, which express GlcNAc6ST-1 but not GlcNAc6ST-2 (9, 40). Furthermore, this binding was eliminated in GlcNAc6ST-1 KO mice,[3] supporting the idea that sulfation mainly occurs on *N*-glycans by GlcNAc6ST-1 in the HEVs of PPs.

S2 significantly inhibited the ear swelling and leukocyte infiltration in CHS responses. Because the antigens recognized by S2 were not expressed at the sites of skin inflammation but were clearly expressed in the draining lymph node HEVs, we think that the reduction of lymphocyte homing into the draining lymph nodes resulted in the reduction in CHS responses. Our results are reminiscent of phenotypes exhibited by L-selectin-deficient (41), FucT-IV and -VII DKO (42), GlcNAc6ST-1 and -2 DKO (9), and C1β3GnT and C2GnT-I DKO mice (8), all of which show reduced CHS responses at least in part because of the reduction of lymphocyte homing into the draining lymph nodes. Taken together, the results of the present and previous studies indicate that manipulating lymphocyte trafficking to reduce lymphocyte homing into draining lymph nodes can reduce CHS responses, suggesting that the newly generated mAbs could serve as therapeutic tools to modulate immune responses in pathophysiological situations.

HEV-like vessels are induced at various sites of chronic inflammation. For example, MECA-79-reactive HEV-like vessels are induced in human gastric mucosa infected with *H. pylori* (32), in ulcerative colitis (33), and in rheumatoid arthritis (43). However, the physiological roles of the sulfated glycans expressed in these specialized blood vessels remain largely unknown. Because one of our mAbs strongly blocked L-selectin-mediated lymphocyte homing in WT mice, it will be useful for examining the roles of sulfated glycans at sites of chronic inflammation in animal models. In addition, because both S1 and S2 bound not only mouse but also human tissues, these mAbs will be useful for assessing the ectopic expression of sulfated gly-

cans in pathophysiological situations, as exemplified in Fig. 10. MECA-79 binds only sulfated extended core 1 *O*-glycans (16) and not sulfated core 2 *O*-glycans or *N*-glycans. In addition, MECA-79 does not recognize terminal sialic acids (16). In contrast, mAb S2 bound sialylated 6-sulfo LacNAc on both *N*- and *O*-glycans and thus can recognize glycan epitopes that are more closely related to the L-selectin-binding sites compared with MECA-79. We thus think that immunohistochemical and functional studies using our mAbs will clarify the roles of sulfated glycans in HEV-like vessels *in vivo*.

In conclusion, our findings demonstrate that anti-carbohydrate mAbs can be efficiently generated by the method described here. Using the newly generated mAbs, we showed that both sulfated *N*- and sulfated *O*-glycans cooperate in lymphocyte homing and immune surveillance, providing a link between carbohydrate structure and lymphocyte trafficking to secondary lymphoid organs under both normal and pathological conditions. Because a number of other studies also indicate that carbohydrates have roles in immunity, studies using anti-carbohydrate mAbs should become increasingly important in this field.

Addendum—While our paper was in the process of being published, Arata-Kawai et al. (44) reported an antibody that also binds sulfated N- and O-glycans similar to S2.

Acknowledgments—We thank Drs. John B. Lowe (Genentech) for providing the FucT-IV and FucT-VII DKO mice, Eugene Butcher (Stanford University, School of Medicine) for providing the MECA-79 hybridomas, and Pamela Stanley (Albert Einstein College of Medicine) for providing the Lec1 and Lec2 cells. We also thank Dr. Yuki Tobisawa and Ryuji Matsumura (University of Shizuoka, School of Pharmaceutical Sciences) for technical support and Core H of the Consortium for Functional Glycomics (funded by National Institutes of Health Grant U54GM62116) for the glycan array analysis.

REFERENCES

1. Varki, A., Cummings, R. D., Esko, J. D., Freeze, H. H., Stanley, P., Bertozzi, C. R., Hart, G. W., and Etzler, M. E. (eds) (2009) *Essentials of Glycobiology*, 2nd Ed., Cold Spring Harbor Laboratory, Cold Spring Harbor, NY
2. von Andrian, U. H., and Mempel, T. R. (2003) *Nat. Rev. Immunol.* **3,** 867–878
3. Butcher, E. C., and Picker, L. J. (1996) *Science* **272,** 60–66
4. Rosen, S. D. (2004) *Annu. Rev. Immunol.* **22,** 129–156
5. Kawashima, H. (2006) *Biol. Pharm. Bull.* **29,** 2343–2349
6. Homeister, J. W., Thall, A. D., Petryniak, B., Malý, P., Rogers, C. E., Smith, P. L., Kelly, R. J., Gersten, K. M., Askari, S. W., Cheng, G., Smithson, G., Marks, R. M., Misra, A. K., Hindsgaul, O., von Andrian, U. H., and Lowe, J. B. (2001) *Immunity* **15,** 115–126
7. Malý, P., Thall, A., Petryniak, B., Rogers, C. E., Smith, P. L., Marks, R. M., Kelly, R. J., Gersten, K. M., Cheng, G., Saunders, T. L., Camper, S. A., Camphausen, R. T., Sullivan, F. X., Isogai, Y., Hindsgaul, O., von Andrian, U. H., and Lowe, J. B. (1996) *Cell* **86,** 643–653
8. Mitoma, J., Bao, X., Petryanik, B., Schaerli, P., Gauguet, J. M., Yu, S. Y., Kawashima, H., Saito, H., Ohtsubo, K., Marth, J. D., Khoo, K. H., von Andrian, U. H., Lowe, J. B., and Fukuda, M. (2007) *Nat. Immunol.* **8,** 409–418
9. Kawashima, H., Petryniak, B., Hiraoka, N., Mitoma, J., Huckaby, V., Nakayama, J., Uchimura, K., Kadomatsu, K., Muramatsu, T., Lowe, J. B., and Fukuda, M. (2005) *Nat. Immunol.* **6,** 1096–1104
10. Uchimura, K., Gauguet, J. M., Singer, M. S., Tsay, D., Kannagi, R., Muramatsu, T., von Andrian, U. H., and Rosen, S. D. (2005) *Nat. Immunol.* **6,** 1105–1113
11. Streeter, P. R., Rouse, B. T., and Butcher, E. C. (1988) *J. Cell Biol.* **107,** 1853–1862
12. Ley, K., and Kansas, G. S. (2004) *Nat. Rev. Immunol.* **4,** 325–335
13. Imai, Y., Lasky, L. A., and Rosen, S. D. (1993) *Nature* **361,** 555–557
14. Hemmerich, S., Butcher, E. C., and Rosen, S. D. (1994) *J. Exp. Med.* **180,** 2219–2226
15. Clark, R. A., Fuhlbrigge, R. C., and Springer, T. A. (1998) *J. Cell Biol.* **140,** 721–731
16. Yeh, J. C., Hiraoka, N., Petryniak, B., Nakayama, J., Ellies, L. G., Rabuka, D., Hindsgaul, O., Marth, J. D., Lowe, J. B., and Fukuda, M. (2001) *Cell* **105,** 957–969
17. Kawano, T., Koyama, S., Takematsu, H., Kozutsumi, Y., Kawasaki, H., Kawashima, S., Kawasaki, T., and Suzuki, A. (1995) *J. Biol. Chem.* **270,** 16458–16463
18. Hiraoka, N., Kawashima, H., Petryniak, B., Nakayama, J., Mitoma, J., Marth, J. D., Lowe, J. B., and Fukuda, M. (2004) *J. Biol. Chem.* **279,** 3058–3067
19. Stamper, H. B., Jr., and Woodruff, J. J. (1976) *J. Exp. Med.* **144,** 828–833
20. Mitoma, J., Miyazaki, T., Sutton-Smith, M., Suzuki, M., Saito, H., Yeh, J. C., Kawano, T., Hindsgaul, O., Seeberger, P. H., Panico, M., Haslam, S. M., Morris, H. R., Cummings, R. D., Dell, A., and Fukuda, M. (2009) *Glycoconj. J.* **26,** 511–523
21. Kannagi, R., Ohmori, K., and Kimura, N. (2009) *Glycoconj. J.* **26,** 923–928
22. Rosen, S. D., Singer, M. S., Yednock, T. A., and Stoolman, L. M. (1985) *Science* **228,** 1005–1007
23. Bierhuizen, M. F., and Fukuda, M. (1992) *Proc. Natl. Acad. Sci. U.S.A.* **89,** 9326–9330
24. North, S. J., Huang, H. H., Sundaram, S., Jang-Lee, J., Etienne, A. T., Trollope, A., Chalabi, S., Dell, A., Stanley, P., and Haslam, S. M. (2010) *J. Biol. Chem.* **285,** 5759–5775
25. Berlin, C., Berg, E. L., Briskin, M. J., Andrew, D. P., Kilshaw, P. J., Holzmann, B., Weissman, I. L., Hamann, A., and Butcher, E. C. (1993) *Cell* **74,** 185–195
26. Gallatin, W. M., Weissman, I. L., and Butcher, E. C. (1983) *Nature* **304,** 30–34
27. Tangemann, K., Bistrup, A., Hemmerich, S., and Rosen, S. D. (1999) *J. Exp. Med.* **190,** 935–942
28. Bruehl, R. E., Bertozzi, C. R., and Rosen, S. D. (2000) *J. Biol. Chem.* **275,** 32642–32648
29. Tobisawa, Y., Imai, Y., Fukuda, M., and Kawashima, H. (2010) *J. Biol. Chem.* **285,** 6750–6760
30. Kawashima, H., Hirakawa, J., Tobisawa, Y., Fukuda, M., and Saga, Y. (2009) *J. Immunol.* **182,** 5461–5468
31. Cummings, R. D., and Kornfeld, S. (1982) *J. Biol. Chem.* **257,** 11230–11234
32. Kobayashi, M., Mitoma, J., Nakamura, N., Katsuyama, T., Nakayama, J., and Fukuda, M. (2004) *Proc. Natl. Acad. Sci. U.S.A.* **101,** 17807–17812
33. Suzawa, K., Kobayashi, M., Sakai, Y., Hoshino, H., Watanabe, M., Harada, O., Ohtani, H., Fukuda, M., and Nakayama, J. (2007) *Am. J. Gastroenterol.* **102,** 1499–1509
34. Lee, J., Park, S. H., and Stanley, P. (2002) *Glycoconj. J.* **19,** 211–219
35. Tahara, H., Ide, K., Basnet, N. B., Tanaka, Y., Matsuda, H., Takematsu, H., Kozutsumi, Y., and Ohdan, H. (2010) *J. Immunol.* **184,** 3269–3275
36. Lasky, L. A., Singer, M. S., Dowbenko, D., Imai, Y., Henzel, W. J., Grimley, C., Fennie, C., Gillett, N., Watson, S. R., and Rosen, S. D. (1992) *Cell* **69,** 927–938
37. Kansas, G. S. (1996) *Blood* **88,** 3259–3287
38. Hoke, D., Mebius, R. E., Dybdal, N., Dowbenko, D., Gribling, P., Kyle, C., Baumhueter, S., and Watson, S. R. (1995) *Curr. Biol.* **5,** 670–678
39. Hiraoka, N., Petryniak, B., Nakayama, J., Tsuboi, S., Suzuki, M., Yeh, J. C., Izawa, D., Tanaka, T., Miyasaka, M., Lowe, J. B., and Fukuda, M.

(1999) *Immunity* **11,** 79–89
40. Uchimura, K., Kadomatsu, K., El-Fasakhany, F. M., Singer, M. S., Izawa, M., Kannagi, R., Takeda, N., Rosen, S. D., and Muramatsu, T. (2004) *J. Biol. Chem.* **279,** 35001–35008
41. Catalina, M. D., Carroll, M. C., Arizpe, H., Takashima, A., Estess, P., and Siegelman, M. H. (1996) *J. Exp. Med.* **184,** 2341–2351
42. Smithson, G., Rogers, C. E., Smith, P. L., Scheidegger, E. P., Petryniak, B., Myers, J. T., Kim, D. S., Homeister, J. W., and Lowe, J. B. (2001) *J. Exp. Med.* **194,** 601–614
43. Michie, S. A., Streeter, P. R., Bolt, P. A., Butcher, E. C., and Picker, L. J. (1993) *Am. J. Pathol.* **143,** 1688–1698
44. Arata-Kawai, H., Singer, M. S., Bistrup, A., van Zante, A., Wang, Y. Q., Ito, Y., Bao, X., Hemmerich, S., Fukuda, M., and Rosen, S. D. (2010) *Am. J. Pathol.*, in press